Key Points:
- Two decades worth of pressure and static fluid level data are compiled from legacy reports for Arbuckle Group injection wells in Kansas
- Arbuckle Group pressures and fluid levels are rising, recently at faster rates, likely associated with increased wastewater injection
- Documented pressure increases explain the recent surge in US midcontinent seismicity

Supporting Information:
- Supporting Information S1
- Table S1
- Table S2
- Table S3
- Table S4
- Figure S1

Correspondence to:
T. S. Bidgoli,
bidgolit@missouri.edu

Accelerated Fill-Up of the Arbuckle Group Aquifer and Links to U.S. Midcontinent Seismicity

E. Ansari[1], T. S. Bidgoli[1,2] (iD), and A. Hollenbach[1]

[1]Kansas Geological Survey, University of Kansas, Lawrence, KS, USA, [2]Department of Geological Sciences, University of Missouri, Columbia, MO, USA

Abstract The Arbuckle Group aquifer is the principal disposal zone for oil and gas field brines and hazardous/nonhazardous wastewater across the U.S. midcontinent and is traditionally viewed as an infinite capacity aquifer. Thousands of wells annually dispose hundreds of millions of barrels of wastewater into the aquifer across Kansas and Oklahoma, but direct links between injection and recent increases in seismicity have been hindered by a lack of pressure data for the Arbuckle Group. Here we present a newly compiled data set for 49 wells across Kansas that provides a unique perspective on the aquifer's performance over two decades. Statistical analysis of falloff test pressures, static fluid levels, and injection volumes shows that Arbuckle pressures and fluid levels are rising, recently at faster rates, likely associated with increased wastewater injection. The new data also suggest that the pressure diffusion, the primary driver of induced seismicity, can reach distances up to 25 km from an injection point and is connected to static fluid level rises. The compiled dataset explains the recent surge in midcontinent seismicity. The data set also suggests that the Arbuckle has finite storage capacity and that wastewater disposal across parts of the midcontinent may soon require alternatives.

1. Introduction

The Cambrian-Ordovician Arbuckle Group (hereinafter the Arbuckle) and its equivalents (e.g., Mount Simon Sandstone in Illinois [Leetaru & Freiburg, 2014], Knox Group in Arkansas [Horton, 2012], Basal Sandstone of the Conasauga Group in Ohio [Nicholson et al., 1988], and Ellenburger Group in Texas [Hornbach et al., 2015]) are used for disposal of oil and gas field brines and hazardous and nonhazardous waste fluid. These deep aquifers are also proposed targets for geologic storage of CO_2 (Benson & Cole, 2008; Bidgoli et al., 2017; Carr et al., 2005; Holubnyak et al., 2017; Schwab et al., 2017). In Kansas and Oklahoma, the Arbuckle is made up of laterally extensive and thick shelf carbonates that are highly permeable and mostly underpressured (Bidgoli et al., 2015; Franseen et al., 2004; Hollenbach et al., 2018), conditions which promote it to readily accept and drain injected fluids by gravity. These characteristics have made the Arbuckle and its equivalents ideal disposal zones across the United States.

Although the Arbuckle has been an industrial wastewater disposal target for more than 70 years (Carr et al., 1986), a surge in seismicity in the midcontinent since 2009, linked to wastewater injection, is challenging assumptions about the safety and longevity of the aquifer for fluid disposal (Hincks et al., 2009; Keranen et al., 2014; Rubinstein & Mahani, 2015; Walsh & Zoback, 2015). The majority of these midcontinent earthquakes, including the four largest events (2016 M 5.8 Pawnee earthquake, 2011 M 5.7 Prague earthquake, 2016 M 5.1 Fairview earthquake, and 2016 M 5.0 Cushing earthquake), have occurred in Oklahoma (Yeck et al., 2017). Seismicity has also spiked in Kansas, with 127 M 3+ earthquakes during 2013–2016 period and the second highest earthquake rate in the central United States (Rubinstein et al., 2018). The bulk of Kansas earthquakes (115 M 3+) have occurred in Sumner and Harper counties in the south-central part of the state, near the Oklahoma border, an area that had only one M 2.0 earthquake prior (Steeples et al., 1990). Earthquake activity has recently increased in central Kansas, since March 2018, with three M 3+ earthquakes occurring near the city of Hutchinson, in Reno County (USGS, 2018). Seismicity in these counties has occurred almost exclusively in the Precambrian crystalline basement, below the Arbuckle (Rubinstein et al., 2018; Schoenball & Ellsworth, 2017), suggesting that the aquifer is hydraulically connected to the deeper basement, where faults are in critical equilibrium and can slip under small stress changes (0.01–0.1 MPa; Reasenberg & Simpson, 1992; Stein, 1999). Pore pressure increases and pressure diffusion are considered the first-order driving mechanism for unclamping these faults and triggering fault slip
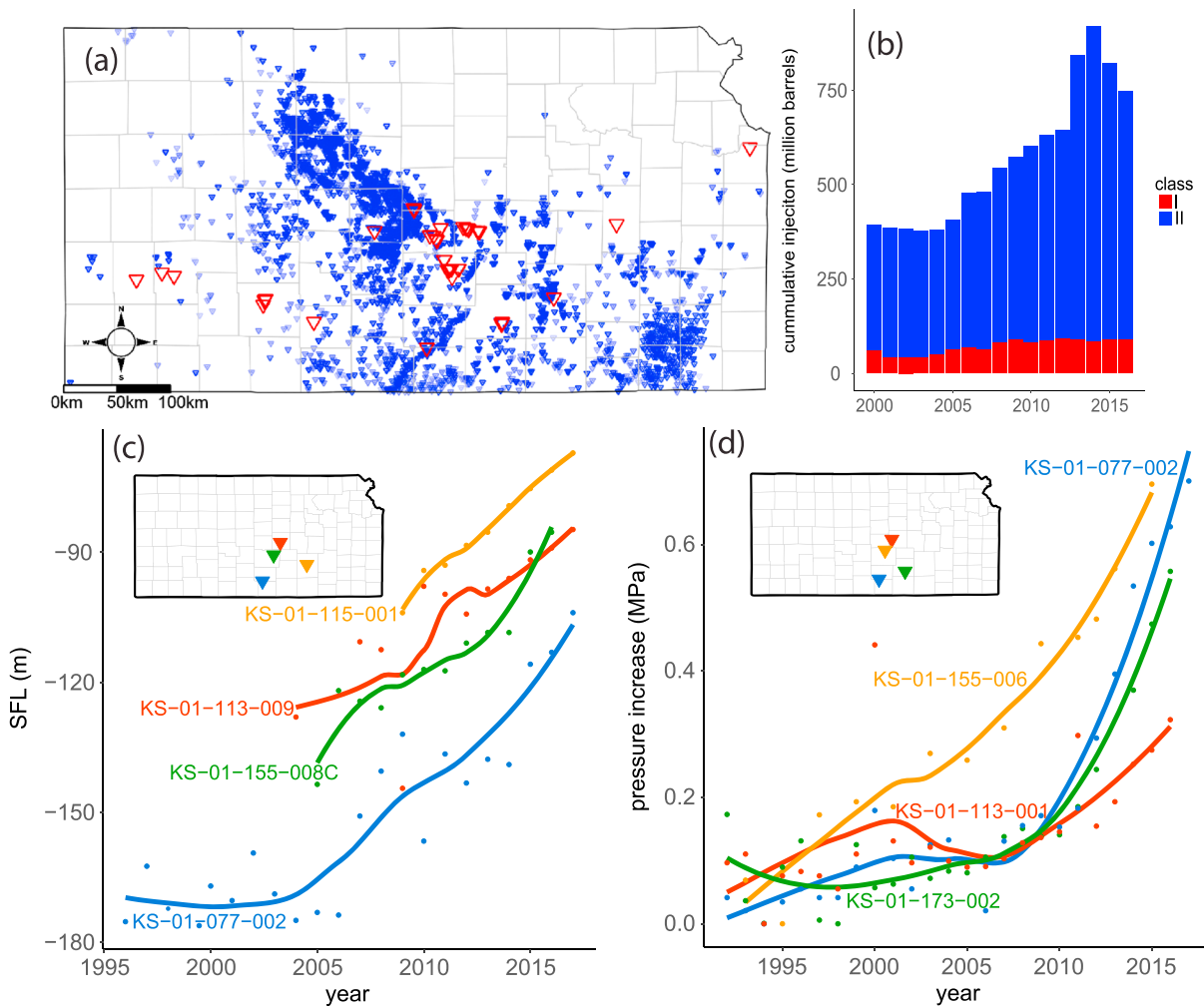
Figure 1. Wastewater disposal wells across Kansas. (a) Locations of 49 Class I wells (red) and 2,381 Class II wells (blue) that dispose wastewater into the Arbuckle Group in Kansas. (b) Yearly wastewater injection volumes from Class I (red) and Class II (blue) wells. Yearly volumes began to increase in 2005, sharply increased in 2013 to >840 million barrels of wastewater, peaked in 2014, with more than 910 million barrels of wastewater injected, and decreased to <750 million barrels in 2016. (c) Example of wells with static fluid levels that are rising toward the surface. Inset map of Kansas shows their locations. The blue line shows well KS-01-077-002, located in northern Harper County where seismicity has increased markedly since 2013. (d) Example of wells with increasing pressure. Well KS-01-155-006 (orange line) has been shut-in for the last two decades; however, its pressure is increasing. Wells KS-01-155-006 and KS-01-155-008C are located near the city of Hutchinson in central Kansas, where seismicity has increased recently. Pressure data (dots) are determined using falloff tests and their trends (solid lines) are determined using locally weighted regression method (see sections 2 and 3). SFL = static fluid level.

(Shapiro, 2015; Shapiro et al., 2013; Segall & Lu, 2015); however, pressure data for the Arbuckle are surprisingly limited, especially given the large number of wells that inject into the zone (Bidgoli et al., 2016; Kroll et al., 2017; Nolte et al., 2017; Schwab et al., 2017).

Wastewater is injected into the Arbuckle using Underground Injection Control Class I and Class II disposal wells. Class I wells refer to the wells that dispose hazardous or nonhazardous industrial fluids, under a strict set of regulations and inspections that include annual pressure falloff tests and static fluid level (SFL) measurements. Class II saltwater disposal (SWD) wells refer to the wells that dispose formation brines coproduced from oil and gas developments. In Kansas, there are 49 Class I and over 2,300 Class II wells that dispose wastewater into the Arbuckle (Figure 1a). These wells are distributed across the state with spatial density of the active wells being higher in the central, south-central, and southeastern parts of the state. Figure 1b shows yearly injection volumes for Class I and Class II wells since 2000. Yearly volumes increased in 2013 to >840 million barrels, peaked in 2014, with more than 910 million barrels of wastewater injected as unconventional oil and gas production increased in the state, and dropped to <750 million barrels per year in
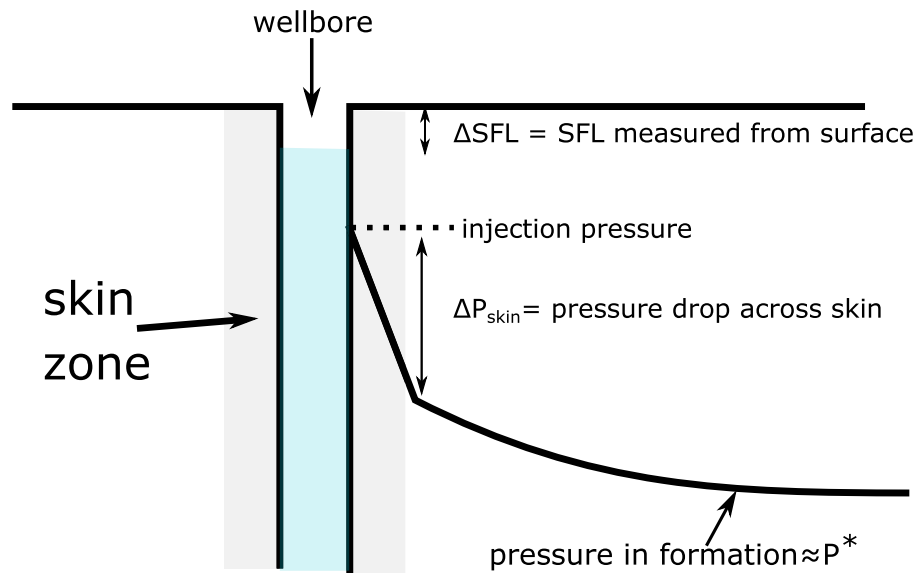
Figure 2. Illustration showing the injection pressure, pressure in the formation ($\approx P^*$), and pressure drop due to skin effect measured by falloff tests. In Class I wells, injection pressure corresponds to the hydrostatic head of the injection fluid (i.e., $\Delta P = \rho g \Delta \text{SFL}$). SFL = static fluid level.

2016, shortly after oil prices fell (Figure 1b). Class I wells alone have injected more than 80 million barrels per year in the last 5 years and account for nearly 13% the total volume of fluid injected into the Arbuckle.

Class I wells, with their stricter well testing guidelines, offer data that can provide insights into the performance of the Arbuckle aquifer with changing injection rates. Recent measurements show an increasing trend for the SFL and pressure of many Class I Arbuckle wells in Kansas (Figures 1c and 1d). The blue line in Figure 1c shows well KS-01-077-002, located in northern Harper County. Wells KS-01-155-006 and KS-01-155-008C are located near the city of Hutchinson. Well KS-01-155-006 (orange line) has been shut-in for the last two decades; however, its pressure is increasing. The increase in pressure and SFL has recently accelerated for many wells across the state (Figures 1c and 1d).

In response to alarming rates of SFL rise in a number of Class I wells and unprecedented seismicity in Kansas and the midcontinent, we compiled more than two decades worth of data from legacy reports for 49 Class I wells to evaluate historical pressures and SFLs in the Arbuckle. The newly assembled data set, combined with Class I and Class II Arbuckle injection volumes, provides a unique perspective on the Arbuckle's reservoir dynamics and storage capacity. In particular, these new data quantify the magnitudes of pressure and SFL increases in the Arbuckle. The new data also suggest that a radius of association between injection volumes and pore pressure changes and confirm the hypothesis that the rising SFLs of the wells and increases in pore pressure are connected. The compiled data set explains the recent surge in midcontinent seismicity. The data set also suggests that the Arbuckle has finite storage capacity and that wastewater disposal across parts of the midcontinent may soon require alternatives.

2. Available Data

Our analysis incorporates data from Class I and Class II wells in Kansas, spanning a 22-year period, from 1995 to 2017. Class I well data were obtained from the Kansas Department of Health and Environment and include injection well locations, yearly injection volumes, and pressures and SFLs that we compiled from legacy reports for required annual well tests and measurements. Class II well data were obtained from the Kansas Corporation Commission and include only the injection well locations and yearly injection volumes. Pressure testing and fluid level measurements are not required under the Underground Injection Control program for Class II wells, thus, such data are quite limited (e.g., Bidgoli et al., 2016; Kroll et al., 2017; Nolte et al., 2017; Schwab et al., 2017; Watney et al., 2016) despite the large number of SWD wells and their substantial injection volumes. The full suite of data is available in the supporting materials (Data Sets S1–S5).
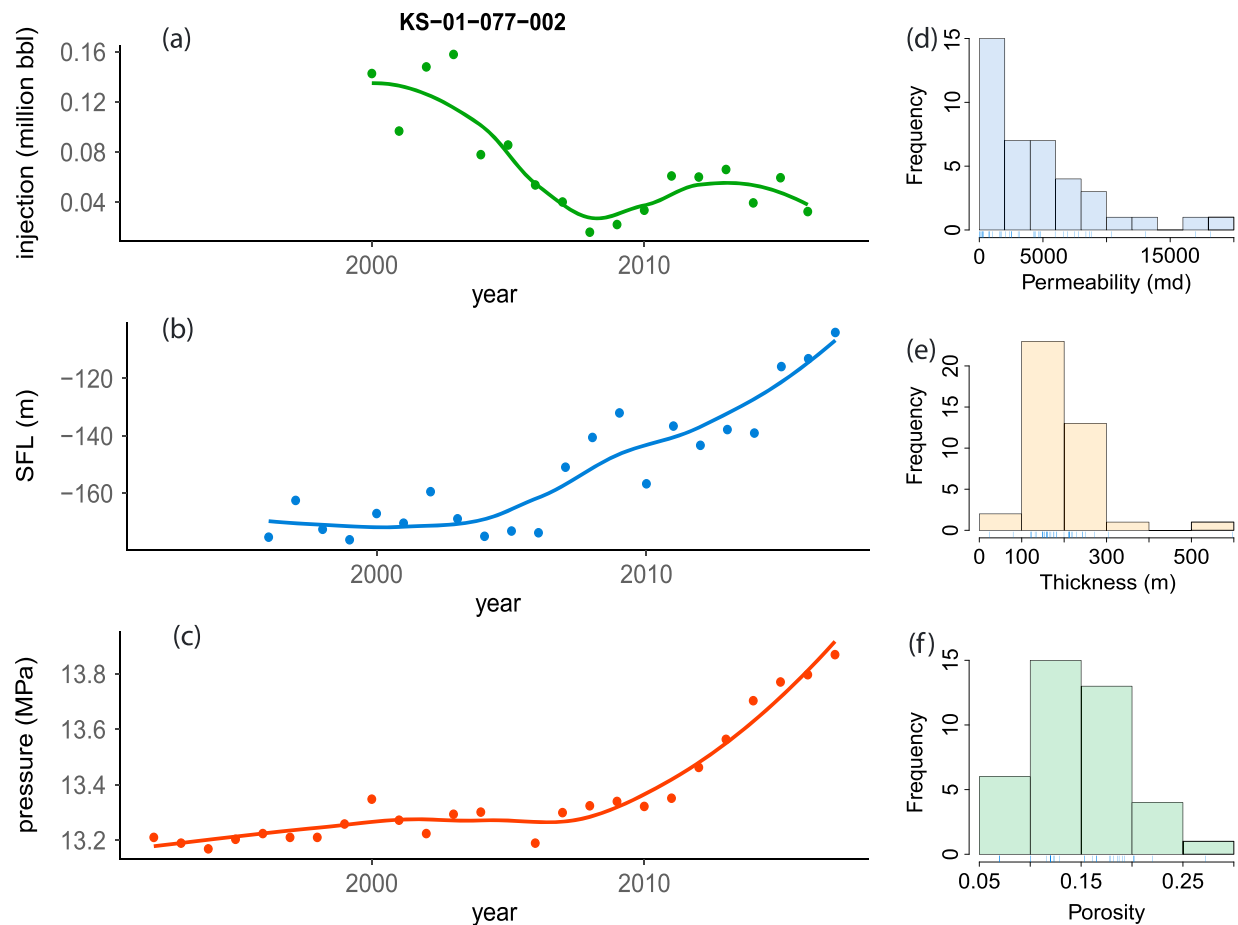
Figure 3. An example of data available for Class I wells (here well KS-01-077-002 located in the northern Harper County). (a–c) Green, blue, and red points show injection volume, SFL, and pressure, respectively. Solid lines show a loess smoothing fit to the data. Both SFL and pressure are increasing while injection remains almost constant in this well, likely the result of injection surrounding the well. (d and e) Arbuckle properties inferred from falloff tests on Class I injection wells. SFL = static fluid level.

For Class I wells, required well tests and measurement provide a wealth of data about the Arbuckle's reservoir properties and performance. However, such data are only available annually because acquiring them is costly for the well operators and requires shutdown of facilities. Well tests and measurements were performed by different operators and contractors, following U.S. Environmental Protection Agency testing procedures (United States Environmental Protection Agency, 2002). The compiled pressures were obtained from 715 pressure falloff tests, used to approximate reservoir pressures (P^*) through Horner analysis (Figure 2; Horner, 1951; see supporting information text for additional details on Horner analysis). Other parameters such as completion interval (reported as the Arbuckle thickness), estimated porosity, and calculated permeability and skin from well test analysis were also tabulated (Figure 2). SFLs (849 in total) were also compiled from reports, and each measurement is the level to which fluid rises after a shut-in well stabilizes and the fluid level becomes stationary, usually measured 24 hr after shut-in. Class I wells inject under gravity (i.e., no wellhead pressure) and their bottom-hole pressure scales with the hydrostatic head of SFL in the well (Figure 2).

Figures 3a–3c show an example of the available data for Class I wells (here well KS-01-077-002). Well KS-01-077-002, the closest Class I well to the Kansas-Oklahoma border, has more than 35-km distance from the border. Figures 3d–3f show the Arbuckle properties inferred from falloff tests on Class I injection wells. It should be noted that all Class I wells have other injection wells (Class I and/or Class II wells) in their vicinity; however, the density of the injectors varies spatially. This spatial variation in well density and injection volumes contributes to the pressure increases and SFL rises observed in each Class I well. The pressure tests
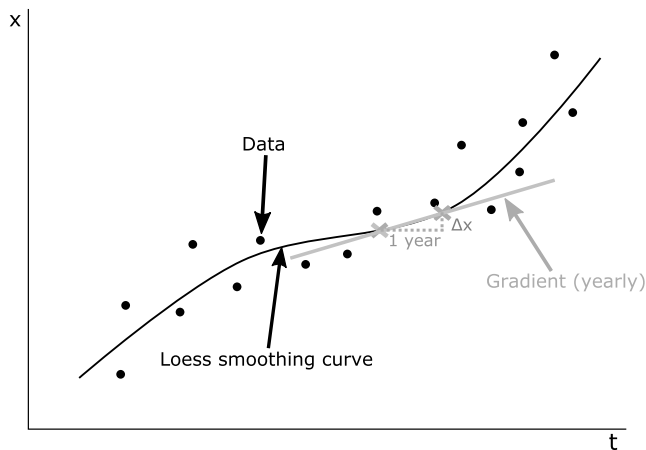
Figure 4. Illustration of calculating the pressure and static fluid level gradients. Locally weighted smoothing curves are fitted to the data, which has a value, x, that varies with time, t, and used to determine trends and gradients.

and SFL measurements are performed independently for the Class I wells and the resulting time series are independent of each other (see supporting information). The injection volumes into Class I wells also vary independently and thus, the total volume injected in the well and within some distance (radius) of the well will have variations.

3. Methods

This work uses simple statistical methods to explore the newly compiled data. The work uses locally weighted regression (also known as locally weighted scatterplot smoothing or loess; Fahrmeir et al., 2013), Pearson correlation coefficients (Mendenhall et al., 2012), and scaling (z score transformation and normalization) to find relationships between the wastewater injection into the Arbuckle, the pressure falloff tests and SFL measurements. All the boxplots used in this study are conventional Tukey boxplots with outliers defined as data that fall below lower fences or above upper fences.

3.1. Locally Weighted Regression

The pressure and SFL have random fluctuations. Locally weighted scatterplot smoothing curves are fit to the dynamic data (pressure and SFL) for each well to obtain the trends in data and calculate temporal gradients (Figure 4). Loess fits remove fluctuations and capture the trends. These smoothing fits are also used for calculating the total increases in the pressures and SFLs.

3.2. Pearson Correlation Coefficient

We use Pearson correlation coefficients (Mendenhall et al., 2012) and corresponding p-values to evaluate bivariate relationships between the pressure/SFL measurements and annual injection volume into each well, annual injection volume within a radius of 5–50 km around each well, and cumulative injection volume into each well and within 5 to 50 km radii. As noted earlier, all of the Class I wells have other injection wells (Class I and/or Class II) surrounding them, with the density of the injectors varying spatially (Figure 1a). For the majority of Class I wells, like those in central Kansas, there are injection wells at each radius surrounding the well and their volumes may be summed or cumulatively aggregated. However, several Class I wells, like those in the far western and eastern parts of the state, may have no other injectors in their immediate vicinity or between two radii (Figure 1a). Figure 5 shows the annual injections rates and cumulative injection within 5 to 35 km radii of well KS-01-077-002 located in the Harper County. Because the Arbuckle is known to be heterogeneous and anisotropic (Franseen et al., 2004) and there are differences among the Class I wells (e.g., perforation length, near-wellbore effects, and injection fluid density), site-to-site comparisons are a challenge. Therefore, we evaluate the correlations between the variables for each Class I well separately and then aggregate the results in boxplots.

3.3. Scaling the Pressure and SFL

Pressures and SFLs have different magnitudes and units. Two scaling methods are commonly used for transforming variables and allowing comparison: standardization (also known as z score transform, equation (1)) and normalization (also known as min-max scaling, equation (2)).
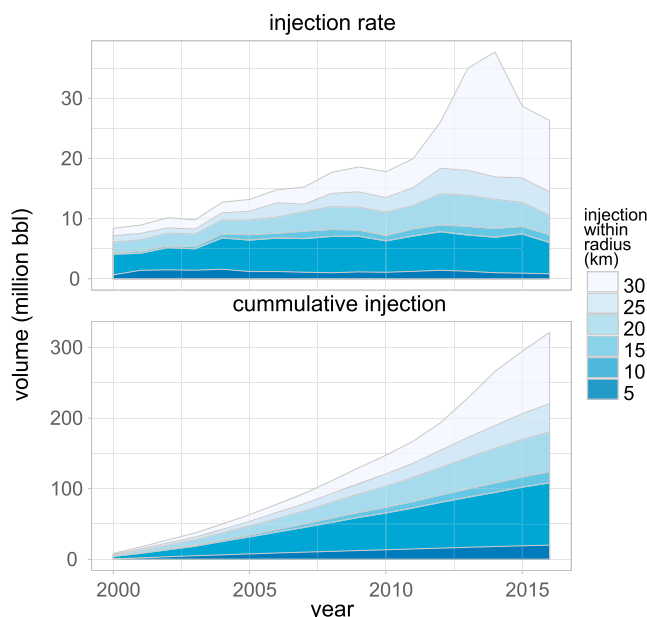

Figure 5. Yearly injection rate and cumulative injected volume within a 5–35 radius of a Class I well (KS-01-077-002).

$$z = x_{\text{standardized}} = \frac{x - \overline{x}}{s_x} \tag{1}$$

$$x_{\text{normalized}} = \frac{x - x_{\min}}{x_{\max} - x_{\min}} \tag{2}$$
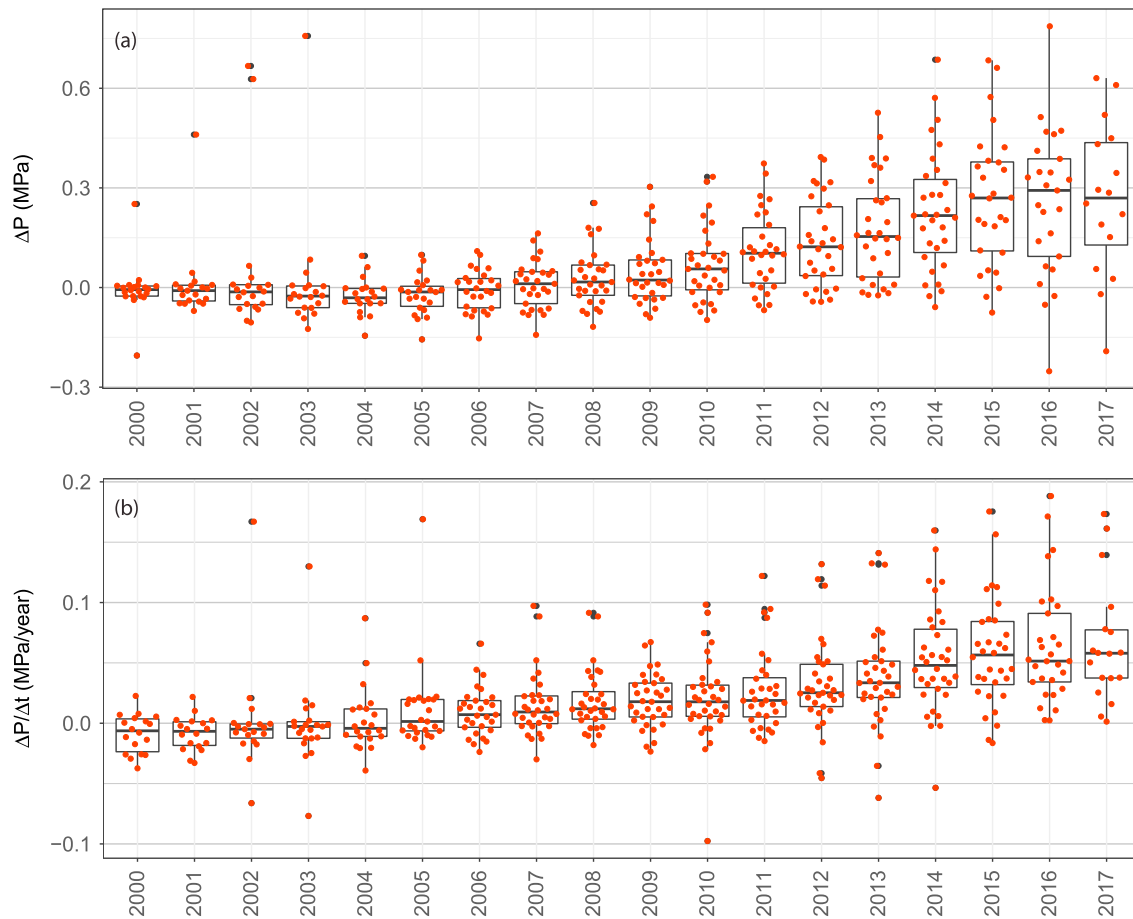
Figure 6. Boxplots of the Arbuckle pressures change (a) and their gradients (b). The rectangles in each year show the first and third quartiles (interquartile range) of the data, the bold line in the rectangle indicates the median, and the bars (whiskers) represent 1.5 times the interquartile range (see supporting information text and Figure S2). The data are jittered on the boxes so that they do not overlap. (a) In 2016, the total pressure increase in the Arbuckle approaches a median of ~0.30 MPa relative to baseline pressure in 1999. (b) The pressure gradient becomes positive in 2006 and increases in 2012 and 2013, accelerating pressure rise and reaching a median of 0.05 MPa/year. The increasing spread in the gradient boxplots show an upper limit of ~0.15 MPa/year for the pressure increase (excluding outliers).

in equation (1), z is the z score, x is the variable (either recorded pressure or SFL vector for each well), and $\bar{x}$ and s_x are the variable mean and standard deviation, respectively. Standardization rescales the data to have a mean of zero and standard deviation of one, and measures how many standard deviation each value lies from a mean of zero. This form of scaling is less sensitive to outliers when compared with normalization (equation (2)), where maximum (x_{max}) and minimum (x_{min}) values are used for scaling, and better suits the current problem in which the data have an increasing trend. We investigate the problem using both scaling methods.

4. Results

4.1. The Magnitude of Increase in Pressures and SFLs

We use locally weighted regression to represent the pressure and SFL for each Class I well and calculate associated gradients and increases relative to a baseline (year 1999 or the first occurrence of data). Figures 6 summarizes the pressure increase (ΔP) and pressure gradient ($\Delta P/\Delta t$) in the Arbuckle using boxplots. Before 2005, the majority of Arbuckle wells show no change or a small reduction in pressure due to slight decreases in injection rates during this period (Figure 6a). In 2006, the pressure gradient (Figure 6b) becomes positive for most wells and pressures start to increase. The gradient in pressure remains constant, with a median of ~0.013 MPa/year, until 2012 and increases or accelerates thereafter with initiation of high-rate injection in
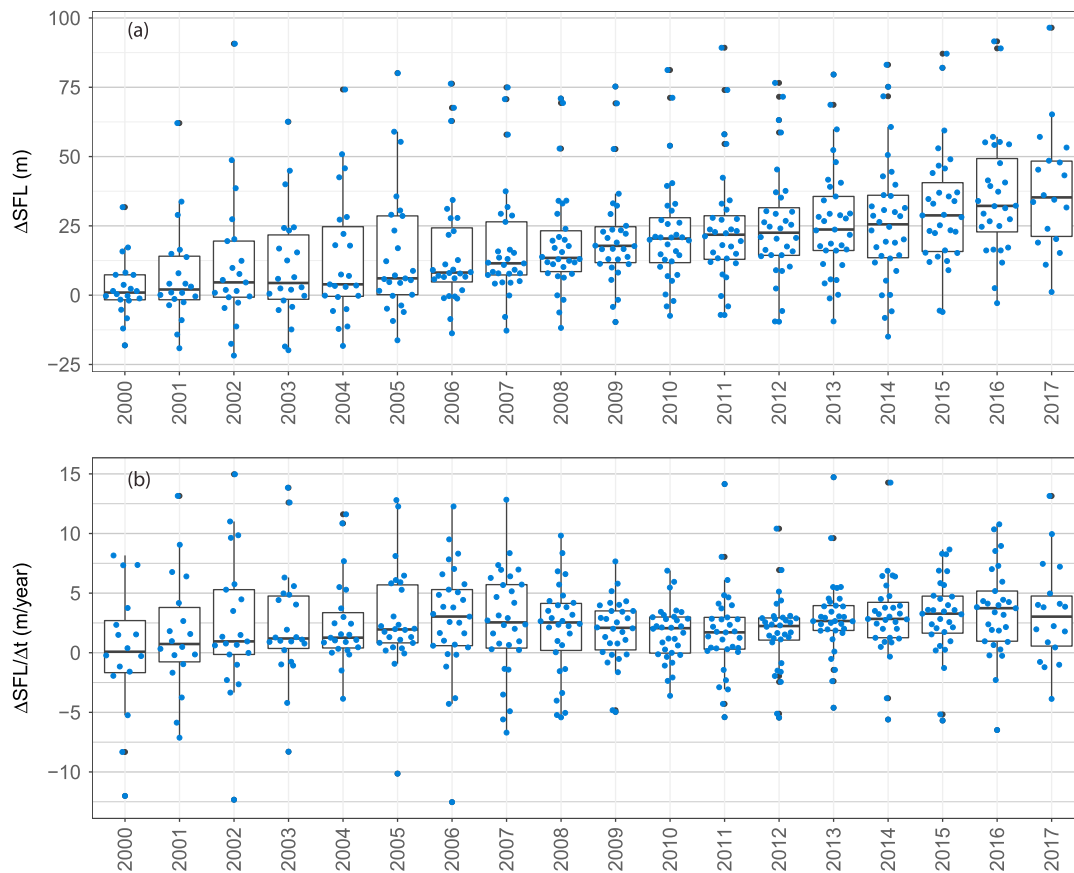
Figure 7. Boxplots of the Arbuckle SFLs (a) and their gradients (b). (a) The pressure gradient becomes positive in 2006 and increases in 2012 and 2013, accelerating pressure rise and reaching a median of 0.05 MPa/year. (b) The SFL gradients are skewed toward zero before 2004 and 2005.75% of wells have a positive SFL gradient in 2004 and 2005. The median SFL gradient increases to more than 2.5 m/year in 2012 accelerating the SFL rise in most wells. The median SFL gradient reaches 3–4 m/year in 2017. The median of total SFL increase in 2017 is ~35 m. SFL = static fluid level.

Class II wells (Figure 6b). In 2015, the rate of increase in the Arbuckle pressure reaches a median of 0.05 MPa/year. In 2017, the total pressure increase in the Arbuckle approaches a median of ~0.30 MPa relative to baseline pressure in 1999. The increasing spread in the gradient boxplots show an upper limit of ~0.15 MPa/year for the pressure increase (excluding outliers).

The SFL rise (ΔSFL) initiated prior to 2005 for more than 50% of wells (Figure 7a), with the median of gradients (ΔSFL/Δt) becoming positive (Figure 7b). After 2005, more than 75% of the wells have a positive SFL gradient. The gradient increases in 2012 and 2013, accelerating the SFL rise in many wells. In 2013, the median SFL increase was 3 m/year, with boxplots comparatively narrow and upper limits reaching 5 m/year. The SFL gradient peaks in 2015 and 2016 and drops in 2017 to a median of ~3 m/year and upper limit of 10 m/year. By 2017, the total increase in the SFL has a median and upper limit of ~35 and 60 m relative to baseline measurements in 1999.

4.2. Factors Affecting Increases in Pressure and SFL

Several parameters can influence the pressure and SFL in wells. Figure 8 shows a pairplot (also known as correlogram; Wright, 2017) of evaluated variables such as pressure, SFL, injection rate, and cumulative injection within several radii for well KS-01-077-002. In this figure, the upper triangle shows the correlation coefficient between the variables, the lower triangle shows the scatterplot and the linear regression fit for the paired variables, and the diagonal shows the associated histogram. The first row in the figure shows the correlation coefficient between SFL and other variables, and the first column shows their corresponding scatter plots. For example, the correlation coefficient between the SFL and pressure, located in the first row and the third column, is 0.87. The correlation coefficients for the wells are extracted from the pairplots and
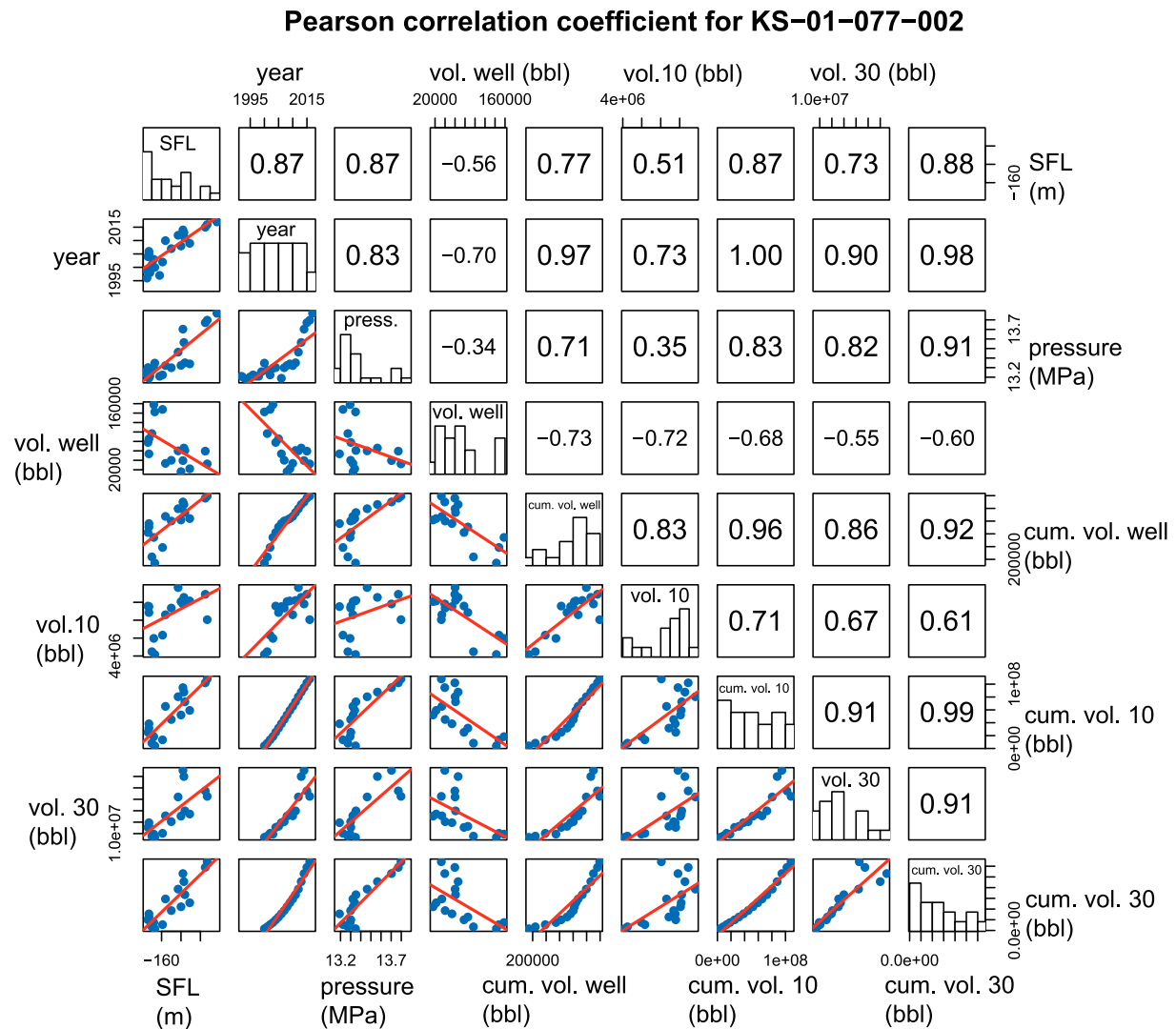
Figure 8. Pairing of the variables for well KS-01-077-002. Upper triangle shows the magnitude of correlation coefficient. Lower triangle shows the scatterplot and linear regression fit for the paired variables. SFL = static fluid level.

aggregated into boxplots (Figures 9a and 9b) to investigate which parameters most strongly correlate with the pressure and SFL.

Figures 9a and 9b summarizes all such boxplots showing the quartiles, median, and the mean (red dot) for the correlation coefficients between the paired variables for all but nine Class I wells (excluded wells had fewer than three pressure or SFL measurements). The pressure shows good correlation (mean, median, and quartiles) with the annual injection rate and cumulative volume injected within a radius of 25 km around the well, a distance beyond which the boxplots remain almost constant (Figure 9a). However, the correlation between the pressure at 25 km and the cumulative volume is stronger that the correlation between the pressure and injection rate at 25 km because change in pore pressure is an additive function and follows pressure superposition principles (Dake, 2008).

SFL, on other hand, shows steadily increasing correlation with the yearly injection rate up to a distance of 25 km from the well, beyond which the boxplots remain almost constant or decrease, but shows the best correlation with the in-well cumulative volume injected (Figure 9b). The difference in observation for SFL compared with pressure is likely related to skin effects and injected fluid density. Near-wellbore porous media acts as a sieve and over time can become clogged, leading to changes in skin that cause pressure increases
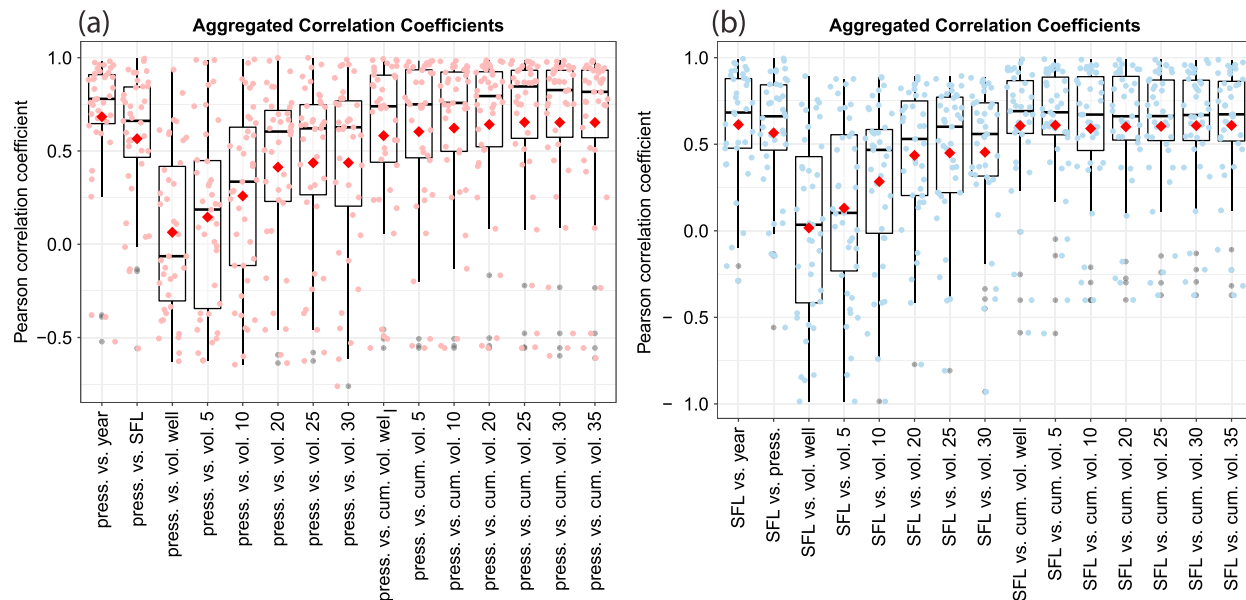
Figure 9. Summary boxplots showing the quartiles, median, and the mean (red dot) for the correlation coefficients between the paired variables (Figure 8) for all but nine Class I wells. Correlation between wastewater disposal and increases in pressures and static fluid levels (SFLs). (a) Boxplot of Pearson correlation coefficients for the pressure paired with other variables. The red dot shows the mean. The correlations increase up a radius of 25 km (comparing first quartile, mean, and median) for both injection volume and cumulative injection volume, with latter having higher correlation. (b) Boxplot of Pearson correlation coefficients for the SFL paired with other variables. The best correlation is between the SFL and cumulative volume injected into the well.

around a well. Differences between the density of the injectate and formation fluid, with the latter a more saturated brine, may also be a factor. As the density of the fluid increases, so does bottom-hole pressure, which drives fluid into formations under gravity drainage. Injection of lower density fluids (i.e., near fresh), as occurs in some Class I wells, can result in higher hydrostatic head and higher SFL.

4.3. Link Between Increases in Pressure and SFL

Though the data suggest that the SFL and pressure may be physically governed by the cumulative waste-water disposal at each well and at 25-km distance from the well, respectively; in practice, calculating and tracking these variables for each well in each year is cumbersome. Additionally, the Arbuckle varies in elevation, pressure, and hydrostatic head across the state, so while many of the wells show similar pressure/SFL trends, scales, and magnitudes are not consistent (trends in pressure/SFL for individual Class I wells are presented in the supporting information). Because the well pressures (and SFLs) have contrasting magnitudes, we scaled the pressure (and SFL) values for each well to their corresponding z-scores (standardization, equation (1)) or between zero and one (normalization, equation (2)) to allow well-to-well comparison while retaining the rank and trend information for the pressure (and SFL) of that well. We then aggregated the scaled pressure (or SFL) for all wells. Figures 10a and 10b show the superimposed pressures (red points) and SFLs (blue points). In these figures, the solid lines show the loess smoothing fits capturing the overall trend in the pressures and SFLs. Both scaling methods show that the pressure increases and SFL rises are correlated and both have increasing trends.

Standardization better suits the current problem because the pressures and SFLs data have an overall increasing trend. Additionally, standardization is less sensitive to outliers compared with normalization in which maximum and minimum values are used for scaling. Thus, we opt to use standardization to develop simple forecast models that can be used to predict increases in pressure and static fluid level for wells in the Arbuckle. These forecast models are based on time (t) because pressure/SFL implicitly depend and have high correlation with time (Figure 9). We also remove the outliers to obtain more accurate forecast models. Univariate boxplots and physical understanding suggest that annual fluctuations of more than 1 MPa in pressure (or 30 m water column height) are likely random effects; therefore, a handful of outliers were removed ($n = 5$) from our analysis to best capture trends.
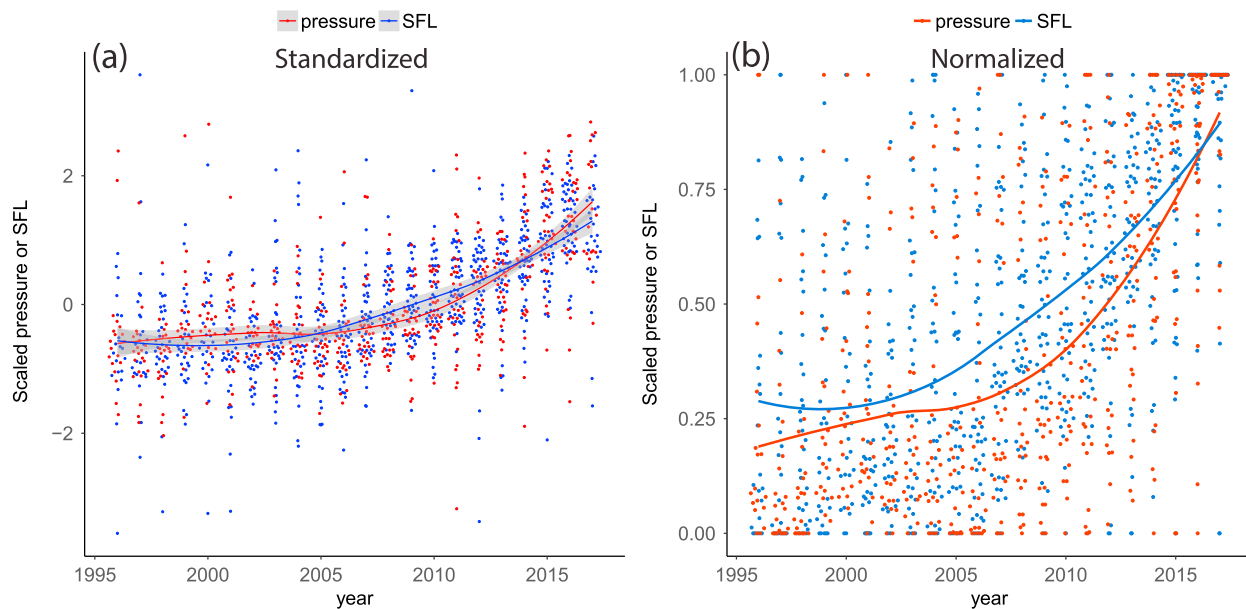
Figure 10. Superimposed pressure and static fluid level. (a) Standardized (z score transform) pressure (red points) and SFL (blue points) are superimposed. Solid lines show loess smoothing fits on the pressure and SFL. (b) Normalized (min-max scaling) pressure (red points) and SFL (blue points) are superimposed. Solid lines show loess smoothing fits on the pressure and SFL. Both scaling methods show that the pressure increases and SFL rises are correlated. SFL = static fluid level.

Figures 11a and 11b present the scaled results and show that most of the Arbuckle wells have an increasing SFL (blue points) and pressure (red points) since about 2005. In these figures, black lines show the loess curves and the gray area represents the 95% confidence interval around the mean. The results suggest that during the late 1990s and early 2000s, the Arbuckle's scaled SFL and pressure were almost constant, and that increases in the scaled SFL and pressure began in 2005 and have accelerated since 2013. These results coincide well with documented increases in disposal volumes into the Arbuckle, which also initiated in 2005 and markedly increased in 2013 (see Figure 1b).

Figures 11c and 11d and Table 1 show two linear approximations for the pressure and SFL after 2005. The first regression line (range [2005–2012]) reflects the increase in the Arbuckle pressure and SFL prior to 2013 and the second regression line (range [2013–2017]) shows the acceleration in the Arbuckle pressure/SFL after high-rate Class II SWD commences in Kansas and Oklahoma. The dashed lines show a forecast for the pressure/SFL if the disposal rate prior to 2013 had continued and can place a lower limit for the coming years. The slope of solid lines for scaled pressure and SFL are close to each other (0.0972 for pressure and 0.1317 for SFL before 2013, 0.2846 for pressure and 0.2286 for SFL after 2013), suggesting that the increases in pressure and SFL are physically connected.

5. Discussion

High-rate injection into the Arbuckle will likely continue as the interest in oil and gas from the Mississippian limestone and other water-rich plays continues across Kansas and the midcontinent. The SFL gradient has been positive for more than 75% of Class I wells since 2005 and most wells show a positive SFL gradient in 2013. The wastewater injection rates in Kansas increased in 2005 and sharply increased in 2013 with the development of the Mississippian limestone and other water-rich plays. Similarly, the rate of pressure and SFL changes in the Arbuckle aquifer increases in 2005 and accelerates in 2013, reflecting this high-volume injection. The data and analyses suggest that the Arbuckle has a finite capacity and limited efficiency for accepting wastewater and exceeding these results in pressure increase and fill-up. Arbuckle fill-up appears to be ubiquitous in Class I wells in central and south-central Kansas, where high volumes of wastewater are being disposed of into the aquifer. With nearly 0.6 MPa increase in pressure and 60 m increase in SFL since 1999, well KS-01-077-002 located in Harper County, is among a few wells in the state to see large increases in both pore pressure and SFL (Figures 1c and 1d) and a concomitant increase in seismicity.
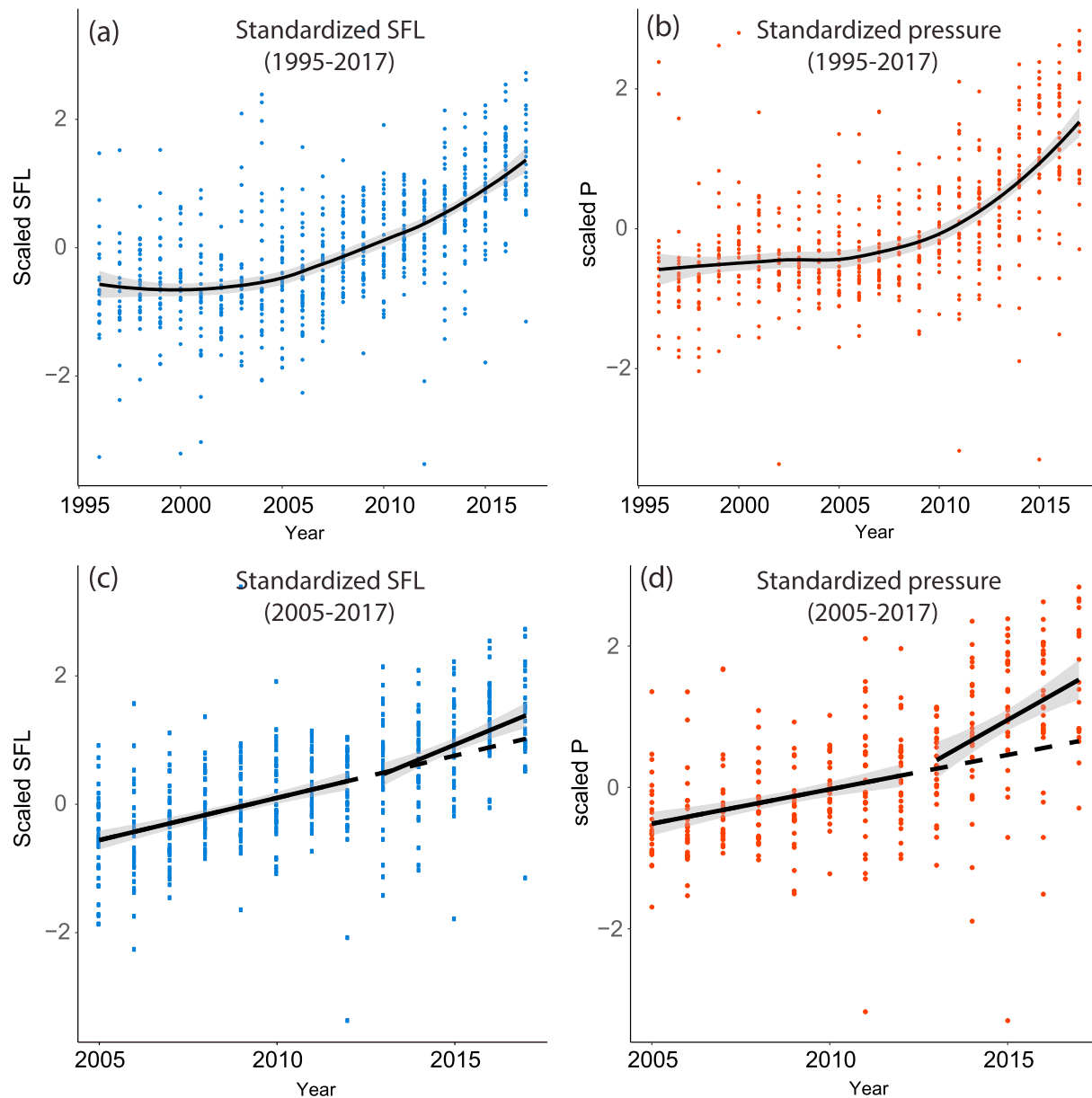
Figure 11. Increases in pressures and SFLs prior to and after 2013. (a and b) The increase in pressure (red points) and static fluid level (blue points). Black lines show the loess smoothing curves and the gray area shows the 95% confidence interval around the mean. Increase in pressure/SFL is evident after 2005 and has accelerated since 2013 when high-rate injection volume has started (see Figure 1b). Pressure and SFL show approximately similar increasing trend. (c and d) These figures show two linear approximation for the pressure/SFL for the range [2005–2012] and [2013–2017]. The first linear regression (range [2005–2013]) shows the increase in the Arbuckle pressure/SFL prior to high-rate wastewater disposal and the second linear regression (range [2013–2017]) shows the increase in the Arbuckle pressure/SFL after high-rate wastewater disposal. The dotted lines show a forecast assuming the pre-2013 disposal rate had continued. SFL = static fluid level.

Wells KS-01-155-008C and KS-01-155-006 (Figures 1c and 1d), located near the city of Hutchinson (where seismicity has increased recently), show a similar pattern. Though a small change in pore pressure (0.01–0.1) in the crystalline basement is enough to reactivate optimally oriented faults (Townend & Zoback, 2000), it appears that a pore pressure change of 0.6 MPa in the Arbuckle is enough to satisfy this condition and trigger M 3+ seismicity. The observed pore pressure change in the Arbuckle is similar to modeled pore pressure changes in the Arbuckle for Oklahoma's Guthrie-Langston earthquake sequence (Schoenball et al., 2018). In addition, Norbeck & Rubinstein, 2018 use analytical solutions and show that pressurization at 3 to 4 km depth where seismicity occurs can reach 25% of the pressurization in the

Table 1
The Equations for Scaled SFL and Pressure Versus Year (Figures 11c and 11d)

Segment	σ_s	p value	Adj. R^2	Years
$SFL_{scaled} = 0.1317\,t - 264.553$	0.68	<0.001	0.16	$2005 < t < 2013$
$SFL_{scaled} = 0.2286\,t - 459.662$	0.72	<0.001	0.16	$2013 \leq t \leq 2017$
$p_{scaled} = 0.0973\,t - 195.6641$	0.67	<0.001	0.10	$2005 < t < 2013$
$p_{scaled} = 0.2846\,t - 572.4276$	0.90	<0.001	0.15	$2013 \leq t \leq 2017$

Note. SFL = static fluid level.

aquifer. Their results fits well with our observation of 0.6 MPa pressure change in the Arbuckle aquifer (or 0.15 MPa in the crystalline basement) can cause M 3+ seismicity. Prior works suggest stress changes of 0.01 to 0.1 are sufficient to trigger fault failure and induce seismicity (Gomberg & Johnson, 2005; Keranen et al., 2014; Rubinstein et al., 2007).

Although increases in pore pressure due to injection are the inferred cause of induced earthquakes, the distance over which disposed fluids are able to affect surrounding faults is uncertain, with previous studies suggesting distances ranging from 10 to 90 km (Davis & Frohlich, 1993; Peterie et al., 2018; Weingarten et al., 2015; Yeck et al., 2016) and some researchers accounting for poroelastic effects (Goebel et al., 2017). Our analysis indicates that a 25 km radius is enough for confidently associating disposal volumes and pore pressure increases in the Arbuckle, a conclusion that suggests other stress transfer processes (e.g., poroelasticity, earthquake-earthquake interaction, and/or aseismic/seismic slip) may be required to explain seismicity at greater distances from injection activity (Cochran et al., 2018; Goebel et al., 2017; Segall & Lu, 2015). A radius of up to 25 km for pore pressure increase is consistent with the observations of Weingarten et al. (2015) who show that the number of associated earthquakes with nearby injection wells remains almost constant at radial distances of 15 to 30 km from the well (Scanlon et al., 2018).

High skin factors reported for some Class I wells (Figure S6) suggest poor connection between the well and surrounding reservoir due to plugged perforations, mud invasion, and/or other factors. The pressure drop near wellbore due to skin effect (i. e., Δp_{skin}) can be reduced by well treatments to increase the injection pressure and mitigate the SFL rises. The Arbuckle aquifer has high permeability and for high permeability reservoirs, high skin factors result in lower pressure drops near the wellbore and may be of little consequence. Large positive skin factors suggest that SFL rises may be mitigated through well stimulation, new perforations, and other treatments that can increase effective wellbore radius (e.g., hydraulic fracturing). These treatments can increase the rate of injection under gravity drainage and can be a short-term solution for wells with high skin factors. However, such treatments are unlikely to change the overall increasing trend in SFL and pressure observed across the Arbuckle and are not a long-term solution because they remove the pressure drop due to skin or increase the wellbore effective radius (in cases of negative skin or hydraulic fracturing) and will not affect the increasing reservoir pressure.

The collected data on the SFL of Class I wells show that Arbuckle fill-up initiated prior to 2005, increased in 2005, and accelerated in 2013, when high-rate injection into the Arbuckle started. The continued rise in SFLs can shut down industrial facilities that do not have alternatives for disposing their wastewater. Although pressure and SFL are measured using different methods, they are correlated, reflecting a single phenomenon, and should be addressed together. Decreasing the injection rate allows for pressure diffusion laterally inside the Arbuckle, and can mitigate the acceleration in pressure/SFL rise. Longer-term solutions for increases in pressure and SFL require reductions in disposal into the Arbuckle and the use of alternative disposal zones.

Our current analysis has two limitations: First, the choice of well testing model for the analysis of pressure falloff tests can change the interpreted results such as aquifer properties (e.g., permeability). The Arbuckle Group is known to be heterogeneous, anisotropic, and fractured. The analysis used by operators for interpreting falloff tests assumes a consistent, isotropic, single-porosity-equivalent aquifer. In the absence of a dual porosity model, the interpreted matrix permeability may be unrealistically large. Second, the measured pressure using falloff tests underestimates the average pressure in the formation and the difference between the measured pressure and average formation pressure increases with time. Thus, the Arbuckle pressure and the changes in pressure are expected to be slightly higher than the values obtained from well test analysis.

6. Conclusions

Two decades worth of data on Class I hazardous/nonhazardous wells injecting into the Arbuckle Group show that the aquifer's pressures are increasing and static fluid levels in the wells are rising. These increases coincide with increases in high-volume wastewater disposal into the aquifer that have accelerated in recent years. The pressure increase has reached a median rate of 0.05 MPa/year and the SFLs rise has reached a

median rate of 3–4 m/year. The results suggest that the Arbuckle Group aquifer has a finite storage capacity and limited efficiency for accepting wastewater, and in certain locations, is filling up. Additionally, the new data and analyses suggest that pressure changes of 0.6 MPa in the aquifer are enough to cause M 3+ seismicity.

Well test data show that the Arbuckle is heterogeneous and has high permeability, which may exert a primary control on spatial and temporal increases in aquifer pressure. Pressure increase is a first-order driving mechanism for induced seismicity and our analysis suggests that such increases can reach distances up to 25 km from the injection well.

Scaled pressures and SFLs have similar increasing trends and are physically connected. While stimulation, hydraulic fracturing, and new perforations can be short-term solutions, a long-term solution for addressing SFL rises is to mitigate the pressure increase by reducing disposal rates into the Arbuckle and allowing the fluid pressures to dissipate. Overall, results from this study suggest that increases in oil and gas production from water-rich plays across the midcontinent may soon require alternatives such as reinjection of wastewater into producing formations or into different disposal zones in near future.

References

Benson, S. M., & Cole, D. R. (2008). CO_2 sequestration in deep sedimentary formations. *Elements*, *4*(5), 325–331. https://doi.org/10.2113/gselements.4.5.325

Bidgoli, T.S., Dubois, M., Watney, W.L., Stover, S., Holubnyak, Y., Hollenbach, A., et al. (2017). Is commercial-scale CO_2 capture and geologic storage a viable enterprise for Kansas? AAPG Datapages/Search and Discovery Article #90309.

Bidgoli, T. S., Holubnyak, Y., & Doveton, J. (2016). Far-field reservoir pressure increases and seismicity in south-central Kansas. *Geological Society of America Abstracts with Programs*. https://doi.org/10.1130/abs/2016AM-286280

Bidgoli, T.S., Holubnyak, Y., and FazelAlavi, M. (2015). Evaluating potential for induced seismicity through reservoir-geomechanical analysis of fluid injection in the Arbuckle saline aquifer, south-central Kansas. AAPG Datapages/Search and Discovery Article #90216.

Carr, J. E., McGovern, H. E., Gogel, T., & Doveton, J. H. (1986). *Geohydrology of and potential for fluid disposal*. Lawrence, KS: Kansas Geological Survey.

Carr, T. R., Merriam, D. F., & Bartley, J. D. (2005). Use of relational databases to evaluate regional petroleum accumulation, groundwater flow, and CO_2 sequestration in Kansas. *AAPG Bulletin*, *89*(12), 1607–1627. https://doi.org/10.1306/07190504086

Cochran, E. S., Ross, Z. E., Harrington, R. M., Dougherty, S. L., & Rubinstein, J. L. (2018). Induced earthquake families reveal distinctive evolutionary patterns near disposal wells. *Journal of Geophysical Research: Solid Earth*, *123*, 8045–8055. https://doi.org/10.1029/2018JB016270

Dake, L. P. (2008). Fundamentals of reservoir engineering. *Environmental Science and Technology*. https://doi.org/10.1016/S0376-7361(08)70005-0

Davis, S. D., & Frohlich, C. (1993). Did (or will) fluid injections cause earthquakes?—Criteria for a rational assessment. *Seismological Research Letters*, *64*(3–4), 207–224. https://doi.org/10.1785/gssrl.64.3-4.207

Fahrmeir, L., Kneib, T., Lang, S., & Marx, B. (2013). *Regression: Models, methods and applications*. Berlin, Heidelberg: Springer Science & Business Media.

Franseen, E. K., Byrnes, A. P., Cansler, J. R., & Carr, T. (2004). *The geology of Kansas: Arbuckle Group*. Lawrence, Kansas: Kansas Geological Survey.

Goebel, T. H. W., Weingarten, M., Chen, X., Haffener, J., & Brodsky, E. E. (2017). The 2016 Mw5.1 Fairview, Oklahoma earthquakes: Evidence for long-range poroelastic triggering at >40 km from fluid disposal wells. *Earth and Planetary Science Letters*, *472*, 50–61. https://doi.org/10.1016/j.epsl.2017.05.011

Gomberg, J., & Johnson, P. A. (2005). Dynamic triggering of earthquakes. *Nature*, *437*. https://doi.org/10.1038/nature04167(7060), 830.

Hincks, T., Aspinall, W., Cooke, R., & Gernon, T. (2009). Oklahoma's induced seismicity strongly linked to wastewater injection depth. *Science*, *7911*, 1–10. https://doi.org/10.1126/science.aap7911

Hollenbach, A., Bidgoli, T. S., Ansari, E., & Nolte, K. A. (2018). Evaluating controls on US midcontinent seismicity through modeling of wastewater injection into the Arbuckle Group aquifer. American Geophysical Union, Fall Meeting, Abstract S31A-02.

Holubnyak, Y., Williams, E., Watney, L., Bidgoli, T., Rush, J., FazelAlavi, M., & Gerlach, P. (2017). Calculation of CO_2 storage capacity for the Arbuckle Group in southern Kansas: Implications for a seismically active region. *Energy Procedia*, *114*, 4679–4689. https://doi.org/10.1016/j.egypro.2017.03.1599

Hornbach, M. J., DeShon, H. R., Ellsworth, W. L., Stump, B. W., Hayward, C., Frohlich, C., et al. (2015). Causal factors for seismicity near Azle, Texas. *Nature Communications*, *6*(1), 6728. https://doi.org/10.1038/ncomms7728

Horner, D. R. (1951). Pressure build-up in wells. *Third World Petroleum Congress The Hague*, 503–521.

Horton, S. (2012). Disposal of hydrofracking waste fluid by injection into subsurface aquifers triggers earthquake swarm in central Arkansas with potential for damaging earthquake. *Seismological Research Letters*, *83*(2), 250–260. https://doi.org/10.1785/gssrl.83.2.250

Keranen, K. M., Weingarten, M., Abers, G. A., Bekins, B. A., & Ge, S. (2014). Sharp increase in central Oklahoma seismicity since 2008 induced by massive wastewater injection. *Science*, *345*(6195), 448–451. https://doi.org/10.1126/science.1255802

Kroll, K. A., Cochran, E. S., & Murray, K. E. (2017). Poroelastic properties of the Arbuckle group in Oklahoma derived from well fluid level response to the 3 September 2016 M w 5.8 Pawnee and 7 November 2016 M w 5.0 cushing earthquakes. *Seismological Research Letters*, *88*(4), 963–970. https://doi.org/10.1785/0220160228

Leetaru, H. E., & Freiburg, J. T. (2014). Litho-facies and reservoir characterization of the Mt Simon sandstone at the Illinois Basin-Decatur project. *Greenhouse Gases: Science and Technology*, *4*(5), 580–595. https://doi.org/10.1002/ghg.1453

Mendenhall, W., Beaver, R. J., & Beaver, B. M. (2012). *Introduction to probability and statistics*. Stamford, CT: Cengage Learning.

Nicholson, C., Roeloffs, E., & Wesson, R. (1988). The northeastern Ohio earthquake of 31 January 1986: Was it induced? *Bulletin of the Seismological Society of America*, *78*(1), 188–217. Retrieved from https://www.bssaonline.org/content/78/1/188.short

Nolte, K. A., Tsoflias, G. P., Bidgoli, T. S., & Watney, W. L. (2017). Shear-wave anisotropy reveals pore fluid pressure–induced seismicity in the U.S. midcontinent. *Science Advances*, *3*(12), e1700443. https://doi.org/10.1126/sciadv.1700443

Norbeck, J. H., & Rubinstein, J. L. (2018). Hydromechanical earthquake nucleation model forecasts onset, peak, and falling rates of induced seismicity in Oklahoma and Kansas. *Geophysical Research Letters*, *45*, 2963–2975. https://doi.org/10.1002/2017GL076562.

Peterie, S. L., Miller, R. D., Intfen, J. W., & Gonzales, J. B. (2018). Earthquakes in Kansas induced by extremely far-field pressure diffusion. *Geophysical Research Letters*, *45*, 1395–1401. https://doi.org/10.1002/2017GL076334

Reasenberg, P. A., & Simpson, R. W. (1992). Response of regional seismicity to the static stress change produced by the Loma Prieta earthquake. *Advancement of Science*, *255*(5052), 1687–1690.

Rubinstein, J. L., Ellsworth, W. L., & Dougherty, S. L. (2018). The 2013–2016 Induced Earthquakes in Harper and Sumner Counties, Southern Kansas. *Bulletin of the Seismological Society of America*, *108*(2), 674–689. https://doi.org/10.1785/0120170209

Rubinstein, J. L., & Mahani, A. B. (2015). Myths and facts on wastewater injection, hydraulic fracturing, enhanced oil recovery, and induced seismicity. *Seismological Research Letters*, *86*, 1060–1067. https://doi.org/10.1785/0220150067

Rubinstein, J. L., Vidale, J. E., Gomberg, J., Bodin, P., Creager, K. C., & Malone, S. D. (2007). Non-volcanic tremor driven by large transient shear stresses. *Nature*, *448*(7153), 579–582. https://doi.org/10.1038/nature06017

Scanlon, B. R., Weingarten, M. B., Murray, K. E., & Reedy, R. C. (2018). Managing basin-scale fluid budgets to reduce injection-induced seismicity from the recent U.S. shale oil revolution. *Seismological Research Letters*, *90*(1), 171–182. https://doi.org/10.1785/0220180223

Schoenball, M., & Ellsworth, W. L. (2017). A systematic assessment of the spatiotemporal evolution of fault activation through induced seismicity in Oklahoma and Southern Kansas. *Journal of Geophysical Research: Solid Earth*, *122*, 10,189–10,206. https://doi.org/10.1002/2017JB014850

Schoenball, M., Walsh, F. R., Weingarten, M., & Ellsworth, W. L. (2018). How faults wake up: The Guthrie-Langston, Oklahoma earthquakes. *The Leading Edge*, *37*(2), 100–106. https://doi.org/10.1190/tle37020100.1

Schwab, D. R., Bidgoli, T. S., & Taylor, M. H. (2017). Characterizing the potential for injection-induced fault reactivation through subsurface structural mapping and stress field analysis, Wellington field, Sumner county, Kansas. *Journal of Geophysical Research: Solid Earth*, *122*, 10,132–10,154. https://doi.org/10.1002/2017JB014071

Segall, P., & Lu, S. (2015). Injection-induced seismicity: Poroelastic and earthquake nucleation effects. *Journal of Geophysical Research: Solid Earth*, *120*, 5082–5103. https://doi.org/10.1002/2015JB012060

Shapiro, S. A. (2015). *Fluid-induced seismicity*. Cambridge: Cambridge University Press.

Shapiro, S. A., Krüger, O. S., & Dinske, C. (2013). Probability of inducing given-magnitude earthquakes by perturbing finite volumes of rocks. *Journal of Geophysical Research: Solid Earth*, *118*, 3557–3575. https://doi.org/10.1002/jgrb.50264

Steeples, D. W., Bennett, B. C., Park, C., Miller, R. D., & Knapp, R. W. (1990). Microearthquakes in Kansas and Nebraska, 1977–89. Kansas Geological Survey Open-File Report, 10–90.

Stein, R. S. (1999). The role of stress transfer in earthquake occurrence. *Nature*, *402*(6762), 605–609. https://doi.org/10.1038/45144

Townend, J., & Zoback, M. D. (2000). How faulting keeps the crust strong. *Geology*, *28*(5), 399–402. https://doi.org/10.1130/0091-7613(2000)28<399:HFKTCS>2.0.CO

United States Environmental Protection Agency. (2002). UIC pressure falloff testing guidelines. Retrieved from https://www.epa.gov/sites/production/files/2015-07/documents/guideline.pdf

USGS. (2018). ANSS comprehensive earthquake catalog (ComCat).

Walsh, F. R., & Zoback, M. D. (2015). Oklahoma's recent earthquakes and saltwater disposal. *Science Advances*, *1*(5), e1500195. https://doi.org/10.1126/sciadv.1500195

Watney, W. L., Bidgoli, T. S., Victorine, J., Simpson, P., Holubnyak, Y., Nolte, K., et al. (2016). Continuous Pressure and Temperature Monitoring in Lower Arbuckle Saline Aquifer in Wellington Field, Sumner County, Kansas – Response to the M5.8 Pawnee Earthquake: American Geophysical Union, Fall General Assembly 2016, Abstract S51E-3166.

Weingarten, M., Ge, S., Godt, J. W., Bekins, B. A., & Rubinstein, J. L. (2015). High-rate injection is associated with the increase in U.S. mid-continent seismicity. *Science*, *348*(6241), 1336–1340. https://doi.org/10.1126/science.aab1345

Wright, K. (2017). corrgram: Plot a Correlogram. Retrieved from https://cran.r-project.org/package=corrgram

Yeck, W. L., Hayes, G. P., McNamara, D. E., Rubinstein, J. L., Barnhart, W. D., Earle, P. S., & Benz, H. M. (2017). Oklahoma experiences largest earthquake during ongoing regional wastewater injection hazard mitigation efforts. *Geophysical Research Letters*, *44*, 711–717. https://doi.org/10.1002/2016GL071685

Yeck, W. L., Weingarten, M., Benz, H. M., McNamara, D. E., Bergman, E. A., Herrmann, R. B., et al. (2016). Far-field pressurization likely caused one of the largest injection induced earthquakes by reactivating a large preexisting basement fault structure. *Geophysical Research Letters*, *43*, 10,198–10,207. https://doi.org/10.1002/2016GL070861